

## Chapter 5

# Transport through DNA: where physics and biology meet

### 5.1 Introduction

In chapter 4 we have discussed the possibility of using organic molecules as spacers for GMR devices. We have shown that it is possible to obtain large GMR ratios as well as asymmetries in the  $I - V$  characteristics that might lead to a diode-effect. In many aspects this is an attempt to reproduce at the nanoscale effects already observed in metallic multilayers or in microscaled devices.

An interesting possibility is to produce all-molecular devices. Based on this idea Bandaru *et al.* [217] have recently shown that it is possible to create logic gates using carbon nanotubes without the need of an external metallic gate. Another interesting idea is that of Cobaltocene molecules as both spin injector and spin detector in molecular spin valves [218]. Finally the transport properties of molecular magnets [219] have been shown to be intrinsically coupled to the internal degrees of freedom of the molecule, most notably to its spin state [220, 221].

A tantalising prospect for nanoscale electronics lies in a seemingly unrelated field: genetics, and in particular DNA research [18, 222].

In all cases described above, be it magnetic molecules or DNA, numerical simulations of electronic transport play an important role in predicting their properties and suitability for possible applications. Most of the systems described above fall into the category of macro-molecules. In other words we must move away from systems comprising only a handful of atoms towards larger organic molecules (still at the nanoscale) which are made of a few hundred constituent particles.

For that reason working with DNA as a possible building block for nanoscale electronics is both exciting and challenging. A computational tool for dealing with these large systems with a high degree of accuracy is necessary.

### 5.1.1 What is DNA?

Deoxyribonucleic Acid (DNA) is a polymeric chain of nucleotides.<sup>1</sup> Each nucleotide has three constituent parts: a phosphorous backbone, a sugar molecule (a pentose in the case of DNA)<sup>2</sup> and a nitrogenated base. The first two are the same for every nucleotide while the nitrogenated base is one of four possible choices: Adenine, Guanine, Thymine and Cytosine. Their structural formulas are shown in figure (5.1). These are aromatic compounds with delocalised  $\pi$  bonds.

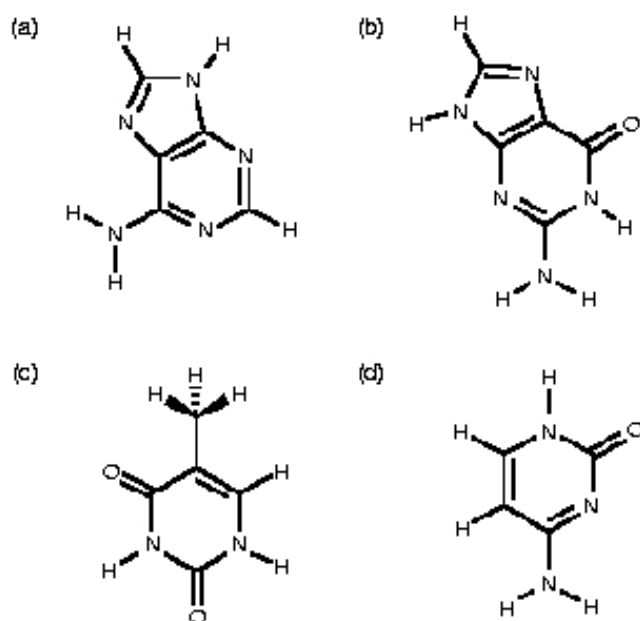


Figure 5.1: Sketch of the four nitrogenated basis that form DNA: (a) Adenine, (b) Timine, (c) Guanine and (d) Cytosine.

The final structural formula of a nucleotide is shown in Fig. (5.2). Nucleotides bond together via hydrogen bonds between the basis to form pairs. Interestingly, although there are four basis, each one can only bond to a single complimentary counterpart.<sup>3</sup> As we can see from figure (5.3) each base pair is coupled through

<sup>1</sup>Nucleotides are also the building blocks of other important biological molecules such as ribonucleic acid (RNA) and molecules associated with energy production and signalling inside a living cell.

<sup>2</sup>A five-carbon sugar.

<sup>3</sup>There are interesting new structures as G4-DNA which can be derived from single strands of DNA. In G4-DNA four Guanine molecules bond in-plane and the subsequent stacking forms a four stranded DNA-like structure (tetra-helix structure). In this work we will only concern ourselves with DNA itself, we refer the reader to the relevant references to G4-DNA [223].

hydrogen bonds; Guanine to Cytosine, Adenine to Thymine. Pairs of nucleotides are subsequently stacked to form a double stranded structure bonded through the phosphate backbone.

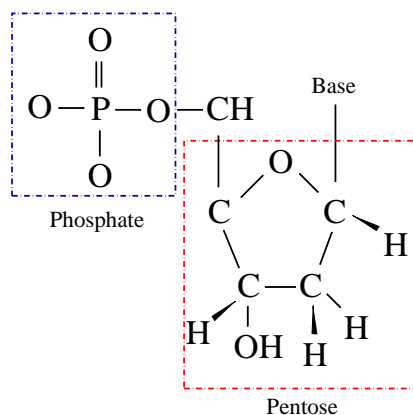


Figure 5.2: Structural formula for a nucleotide showing the phosphate backbone and the pentose. The base is one of (a-d) in figure (5.1).

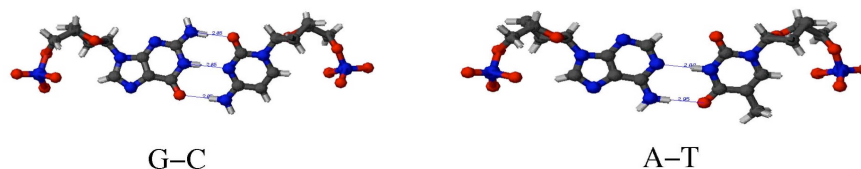


Figure 5.3: The molecular selectivity properties of DNA nitrogenated basis'; the hydrogen bond coupling of (a) Adenine to Thymine and (b) Guanine with Cytosine. Colour code: white - hydrogen, grey - carbon, red - oxygen, blue - nitrogen and dark blue - phosphorus.

Furthermore, because strands of the backbone are aligned anti-parallel to each other the planar stacking of these aromatic compounds is at an angle. This leads to a helical structure. Such an arrangement was first proposed by Watson and Crick [224] based largely on x-ray data by Franklin [225] and Wilkins [226]. Their work was considered so important that Watson, Crick and Wilkins were awarded the Nobel prize in Physiology or Medicine in 1962 [227].<sup>4</sup> The structure shown as a ball-and-stick model in Fig. (5.4) - the structure of DNA - is probably the most recognisable image in the biological sciences today.

<sup>4</sup>Until Watson and Crick's proposal the structure of DNA was one of the most sought after results in crystallography and the biological sciences. Models had been proposed by Pauling and Corey [228, 229] as well as others. For an interesting yet highly personal and one-sided account of the discovery of the DNA structure one should refer to Ref. [230]

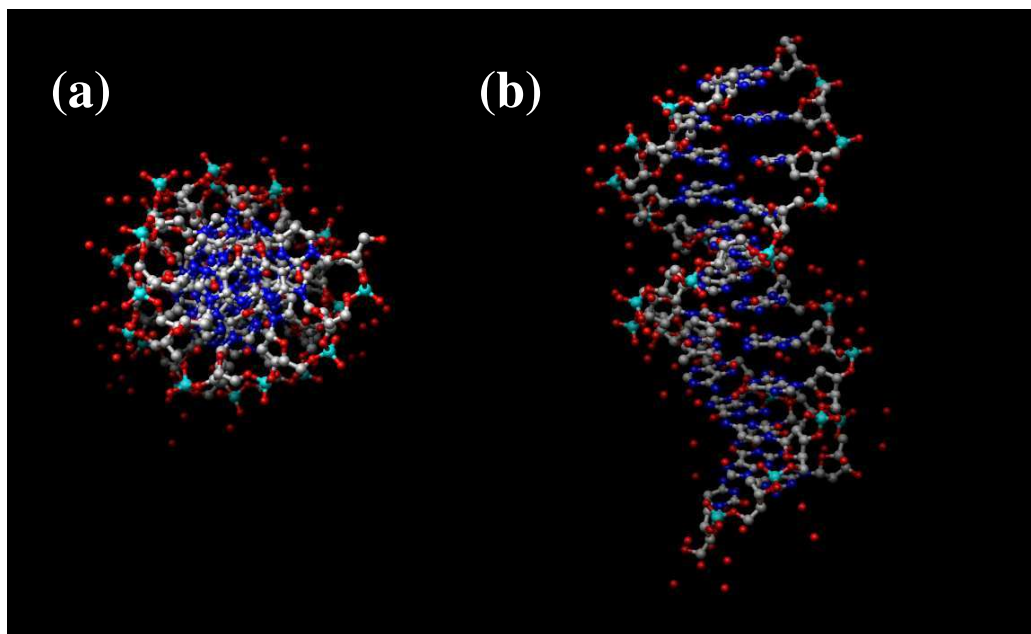


Figure 5.4: (a) Side and (b) top views of one full turn (10 base pairs) for B-DNA. Red spheres following the backbone denote possible counter-ions. Colour code: white - hydrogen, grey - carbon, red - oxygen, blue - nitrogen and cyan - phosphorus.

The arrangement of the atoms in a DNA molecule can be done in different ways while retaining the double helix structure (the main signature of a DNA molecule). The two main forms of DNA we are interested in are known as A-DNA and B-DNA [231, 232, 18]. B-DNA is found under physiological conditions, *i. e.*, in the presence of water molecules and when humidity levels are above 90 % [18]. When humidity levels drop below 75 % we have dry DNA and the structure of the molecule changes into the A form. In figure (5.4a-b) we show side and top views for one full turn of B-DNA and in Fig. (5.5a-b) we have the same for A-DNA.

We can note that the atomic arrangements are significantly different. Firstly, the stacked nitrogenated basis are aligned perpendicular to axis of the helical structure in B-DNA and at an angle in the case of A-DNA. Secondly, the twisting angle has also changed. In the case of B-DNA the angle between stacked base-pairs is  $36^\circ$  whereas in A-DNA it is  $32.7^\circ$ . This means that we need ten base pairs in the former case and eleven in the latter in order to have one full turn of the double helix structure (a periodic cell) in the solid state sense.

The interest in DNA from a biological perspective arises because it contains the complete information about each living being, *i.e.* it regulates the transcription of

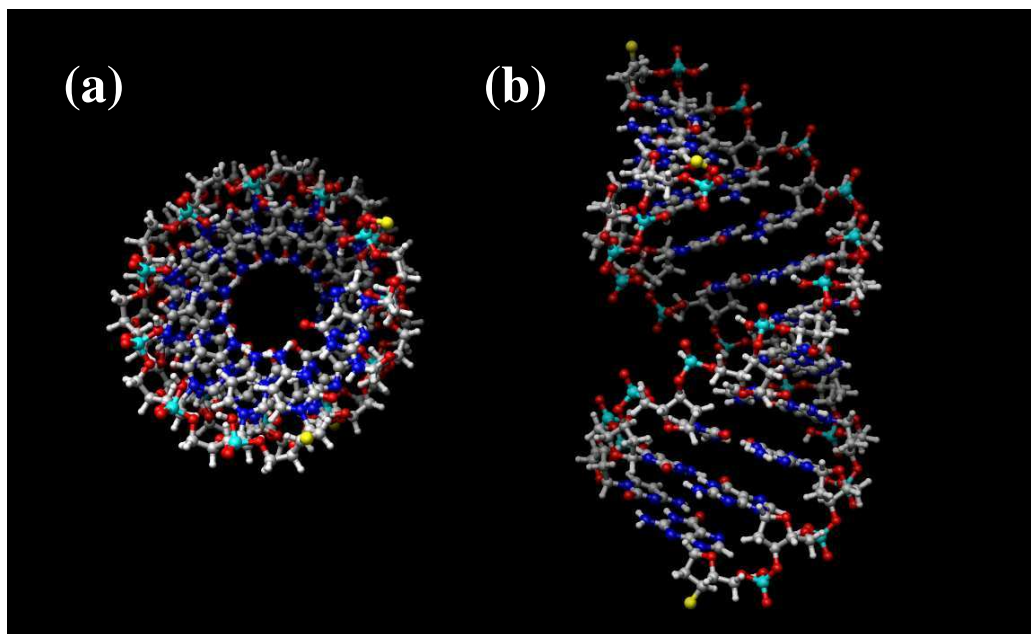


Figure 5.5: (a) Side and (b) top views of one full turn (11 base pairs) for A-DNA. The water molecules and counter-ions have not been included. Colour code: white - hydrogen, grey - carbon, red - oxygen, blue - nitrogen and cyan - phosphorus. The yellow spheres denote the sulphur atoms which anchor the molecule to a metal. In infinite strands it is not present.

proteins which are responsible for our metabolism. It also determines our physical appearance and many aspects of our health. In essence DNA can be considered as the ultimate memory device. Understanding the structural and functional aspects of this molecule has led to a number medical breakthroughs and a deeper understanding of living organisms as a whole [233]. Although a great deal has been done in that aspect an insurmountable amount of work still remains and there many exciting questions remain unanswered [233].

### 5.1.2 Is DNA a conductor?

But why are physicists and materials' scientists interested in DNA for electronics applications? One of the reasons is due to its molecular recognition properties. In other words its ability to bond with specific molecules (Guanine to Cytosine and Timine and Adenine) can lead to self-assembled devices at the molecular level.

Braun *et al.* [19] explored this idea by attaching different types of nucleotide sequences to two separate gold electrodes. These single stranded oligonucleotides

work as hooks, while in mean time,  $\lambda$ -DNA<sup>5</sup> is deposited in solution onto the sample. The 16- $\mu$ m-long  $\lambda$ -DNA then hybridises with specific nucleotides; only those which provide a specific matching combination. Subsequently the authors coat the DNA molecule which has attached to the electrodes with Ag clusters, using the DNA strands as a template for metallic interconnects.

One can clearly see the amazing possibilities. Integrated circuits can be designed by marking electrodes with a specific (or combination of) basis. The desired connections are immediately made once DNA in aqueous solution is deposited onto the sample.

More interestingly still is whether it would be possible to use DNA itself as the device instead of merely as a template. This in turn leads to the issue of DNA conductivity. This is no doubt a contentious one.

The first proposal in favour of DNA conductivity was made as early as 1962 by Eley and Spivey [234]. The authors proposed that the  $\pi - \pi$  bonds between stacked basis could create a delocalised state along the double helix that would lead to conducting behaviour. Indeed, other similar stacked aromatic crystals present metallic character [235], although some crucial differences with DNA are evident. Most notably DNA is not, strictly speaking, a polymer because the arrangement of the stacked basis is not necessarily periodic. This can possibly lead to localisation effects which might hinder the conduction.

Unfortunately, experimental results so far seem unable to answer this question unambiguously. Braun *et al* [19] in their work on DNA-templated metallic wires measured the conductance of 11- $\mu$ m-long DNA molecules deposited on a glass substrate and sulphur-bound to gold electrodes. They show that DNA in solution (B-DNA) is insulating up to 10 Volts of externally applied bias; no conductance is seen over this bias range. This result seems to suggest that DNA is insulating. Experiments performed by de Pablo *et al.* [236] also show no conductance (resistances of at least  $10^{12} \Omega$ ) on 1- $\mu$ m-long  $\lambda$ -DNA double strands deposited on mica surfaces.

In contrast, Fink *et al.* [21] used a low-energy electron point source (LEEPS) to image bundles of DNA molecules approximately 600 nm long. These ropes were deposited on a conducting sample holder with holes. The measurements were then performed using a manipulating tip that approaches the bundles until contact is made. The  $I - V$  characteristics suggest that DNA conducts as efficiently as a good semiconductor (its behaviour is Ohmic). However, these results have been challenged

---

<sup>5</sup> $\lambda$ -DNA is simply the genetic material of the bacteriophage virus *Enterobacteria phage*  $\lambda$ . It can be easily isolated in the laboratory and therefore is a good candidate in experiments. In our work, for practical purposes we consider  $\lambda$ -DNA simply as a random sequence of nucleotides.

by de Pablo *et al.* [236]. It has been argued that even the low-energy electrons used in the imaging process can cause damage to the DNA structure and lead to higher conductivity.

Kasumov *et al.* [237] obtained some striking results. They suggested that DNA deposited on Re/C electrodes on a mica substrates is metallic down to 1K - of the order of one resistance quantum. Below such temperature the Re/C contacts undergo a superconducting transition and the DNA molecules become superconducting as well due to proximity effect. Since these results have never been reproduced, we should consider them the least reliable ones and we shall not address them here.

This brings us to the last set of results for conductivity in DNA. Experiments on short DNA strands (between 26-30 base pairs) were performed by Porath *et al.* [20] and subsequently by Cohen *et al.* [238, 239]. In both cases, the authors performed conduction experiments on short suspended DNA strands - between 26 and 30 base pairs. Porath and collaborators used a suspended Platinum bridge with an 8 nm gap where a 10.4-nm-long poly(G)-poly(C) DNA oligomer was deposited. The corresponding  $I - V$ 's present a voltage gap that varies from sample to sample from about 1.5 up to 2.5 Volts and the currents obtained were about 1.5 nA at 4 Volts. Cohen *et al.* took this experiment further by depositing a thin film of DNA short strands 5'-thiolated on both ends on a single gold substrate. Subsequently a gold nanoparticle is allowed to bond to the remaining sulphur at the other end of the strand. The authors then use a conducting AFM tip to measure the conductance of, what the authors claim is, a single DNA molecule. The results show the same voltage gap from the previous experiment, but much higher currents: of the order of 100 nA even in the case of complex nucleotide combinations. Besides double stranded DNA (dsDNA) the authors also considered single stranded (ssDNA) and systems where the sulphur anchoring group was removed. In all cases except for dsDNA bonded through S groups no conducting behaviour was observed. Finally, in both articles, the authors suggest that transport is mediated by molecular energy bands and that DNA behaves as a wide-gap semiconductor.

More recently Xu and coworkers [23] performed break junction experiments on DNA molecules in aqueous solution (the molecules were shorter, containing only 8 base pairs). Their results show no conductance gap and also high currents.

Other experiments deal with charge transfer in free standing (in the absence of electrodes) DNA molecules in solution. For these experiments, an electron is photo-excited and allowed to relax. It is usually accepted that the excited electrons move towards guanine nucleotides which are regarded as acceptors [240, 241]. In these

experiments a number of mechanisms have been proposed for the observed charge transfer depending on the energetics of the of the base sequence [242, 243, 244, 245]. These experiments are conceptually different to direct conductance measurements where the molecule is contacted between two electrodes (a source and a drain) and an external bias is applied. According to Porath *et al.* [20] none of the mechanisms for these setups can account for the results in direct conductance measurements.

At first it appears that the plethora of results shed no light on our initial question. But if we take a closer look, we will see a general picture arising from these seemingly conflicting conclusions. The experiments that show low conduction or insulating behaviour were performed on mica or glass surfaces. It has been shown that the interaction with the substrate leads to significant changes in the DNA molecule [246]. Most importantly, results showing semiconductor behaviour were obtained in short DNA strands (between 8-30 base pairs). These observations suggest that at these length scales the electronic transport is coherent, whereas for larger length scales (the micrometre range) inelastic effects may dominate.

Some theoretical work has been performed on DNA molecules. Taniguchi and Kawai [247] performed DFT calculations on A- and B-Poly(dA)-Poly(dT) and A- and B-Poly(dG)-Poly(dC) molecules.<sup>6</sup> The authors showed that the HOMO in both A and B forms is largely adenine- (for Poly(dA)-Poly(dT)) or guanine-dominated (for Poly(dG)-Poly(dC)). De Pablo *et al.* [236] also performed DFT calculations on a periodic Poly(dG)-Poly(dC) A-DNA molecule. In this case the authors also considered base swaps at a concentration of one per every 11 pairs to show the effects of Anderson localisation and to argue that random DNA sequences are insulating.

Endres *et al* [248] have performed DFT calculation to show that the effective coupling between stacked basis is close to zero in the case of A-DNA and up to 0.1 meV for B-DNA. Firstly, this results show that the twisting angle has an influence on the inter-base coupling along the helix. Secondly, in principle, one should expect little or no conductance even in the case of a periodic double strand because the state at the Fermi level can be considered as a collection of isolated molecular orbitals for the base pairs.

All these calculations were performed using standard equilibrium DFT. The effects of the electrodes have been completely neglected and the conductivity can only be inferred by looking at the band structure. Transmission curves or  $I - V$  characteristics thus far have only been calculated with model Hamiltonians [249].

---

<sup>6</sup>A periodic sequence of adenine-thymine (Poly(dA)-Poly(dT)) or guanine-cytosine (Poly(dG)-Poly(dC)) base pairs.



One important issue that has been neglected in all previous DFT calculations is the role of the electrodes. The alignment of the molecular orbitals with the Fermi level of the semi-infinite leads will greatly influence the transport properties of these systems.

## 5.2 Calculations

Fully *ab initio* transport calculations on DNA, although computationally demanding, seem to be the only way of unambiguously assessing the conductivity of DNA molecules. *Smeagol* is the perfect tool for this task, being fully parallelised and capable of treating systems in excess of 1000 atoms (see section 2.4.1).

In all our calculations the DNA molecule was modelled using the following basis set

Atom	<i>s</i>	<i>p</i>	<i>d</i>
H	1 <i>s</i> <sup>1</sup> DZ	-	-
C	2 <i>s</i> <sup>2</sup> DZ	2 <i>p</i> <sup>2</sup> DZ	-
N	2 <i>s</i> <sup>2</sup> DZ	2 <i>p</i> <sup>3</sup> DZ	-
O	2 <i>s</i> <sup>2</sup> DZ	2 <i>p</i> <sup>4</sup> DZ	-
P	3 <i>s</i> <sup>2</sup> DZ	3 <i>p</i> <sup>3</sup> DZP	-
S	3 <i>s</i> <sup>2</sup> DZ	3 <i>p</i> <sup>3</sup> DZP	3 <i>d</i> <sup>0</sup> SZ
H'	1 <i>s</i> <sup>1</sup> DZP	-	-
O'	2 <i>s</i> <sup>2</sup> DZ	2 <i>p</i> <sup>4</sup> DZP	-
N'	2 <i>s</i> <sup>2</sup> DZ	2 <i>p</i> <sup>3</sup> DZP	-

Table 5.1: Initial atomic configurations and their respective basis sets for each element in the DNA calculation. Elements denoted by prime are involved in hydrogen bonds.

For those atoms where H-bonds are involved we use extra polarisation orbitals: *s* orbitals in hydrogen and *p* orbitals in nitrogen and oxygen. This basis is the same used in previous calculations [236, 250] with satisfactory results.

We considered two DNA molecules both in the A form, namely a molecule containing 2 base pairs and another one containing 11 base pairs (one full turn of the double helix structure). The molecules are attached on the hollow site of two gold [001] surfaces via thiolate end-groups. Figure (5.6) shows ball-and-stick models of these two arrangements. The gold electrodes were modelled as 10x5x4 finite clusters (the introduction of self-energies turn them into semi-infinite quasi-1D wires). For the gold atoms bonded to the S end-groups we used *s*, *p* and *d* in the valence with

a double- $\zeta$  basis and soft-confinement potentials [40]. For the remaining gold atoms we use a single  $5s$  orbital and we placed the filled  $d$  orbitals in the core.

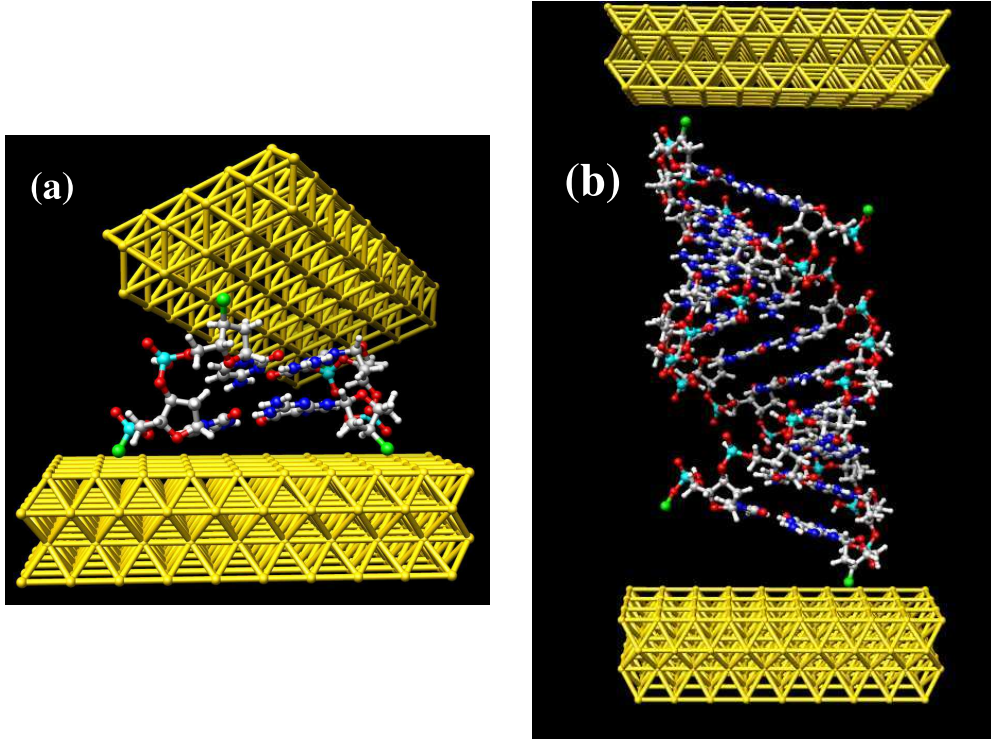


Figure 5.6: Ball-and-stick model of a) a two-base-pair, and b) an eleven-base-pair A-DNA arrangements. Color code: Au - gold; C - grey; H - white; O - red; N - blue; P - cyan; S - green

### 5.2.1 Describing Au in DFT with $s$ orbitals only

In the case of bulk gold, LDA gives a good description of the electronic properties if we include the filled  $5d^{10}$  and half filled  $6s^1$  states in the valence and the remaining filled orbitals in the core (described by the pseudopotential).<sup>7</sup>

Figure (5.7a) shows the band structure along symmetry lines for a fully converged calculation of bulk gold at the DFT equilibrium lattice constant (4.09 Å) with a rich basis set (double- $\zeta$  with soft-confinement potentials). We can see that the Fermi level, as it would be expected, is largely dominated by a broad  $s$  band. The  $d$  and  $p$  orbitals start to play a role at energies 3 eV below and 3 eV above  $E_F$  respectively.

The inclusion of  $5d$  and  $6p$  orbitals in the gold electrodes of our DNA transport calculation would make the problem intractable since the total number of basis func-

<sup>7</sup>The atomic configuration of Au is [Xe]  $4f^{14} 5d^{10} 6s^1$ .

tions will exceed the amount of memory available. Fortunately the description of the leads in the transport problem depends largely on the band structure which are much more resilient basis set choice than total energy calculations. In other words, the band structure of the electrodes can be satisfactorily described by a simpler basis set without sacrificing the overall precision.

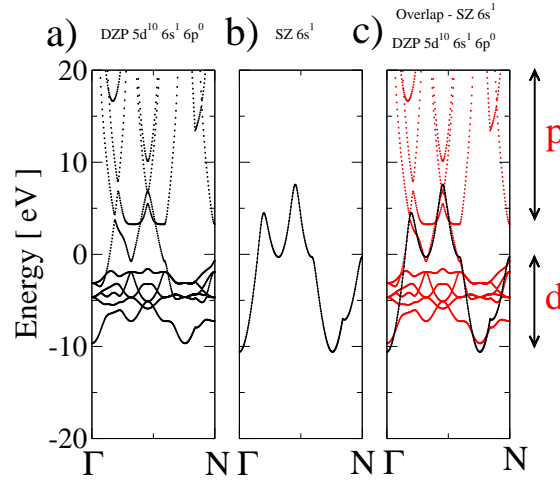


Figure 5.7: Band structures obtained using SIESTA with different types of basis sets and pseudopotentials for gold. a) double- $\zeta$  *spd* with polarisation orbitals, b) single zeta *s* with core correction and c) graphs (a) - red - and (b) - black - have been superimposed to show the similarity.

In fact, we performed band structure calculations (shown in Fig. (5.7b-c)) where the *5d* orbitals were included in the core. We can clearly see that the band structures for this simpler case is very similar to the more precise calculation in the region  $\pm 3$  eV around  $E_F$ . Therefore, for voltages within this window we can expect adequate results.<sup>8</sup> On the other hand, the description of the DNA molecule itself whose transport properties we are calculating is done in an accurate way, *i.e.* with a much richer basis set.

### 5.2.2 Infinite DNA strands

Before we actually start looking at the transport properties of double stranded DNA molecules attached to external leads it is interesting to consider the isolated molecule (without the effects of the electrodes). In figure (5.8) we show the total density of states and the PDOS projected onto the Guanine and the Cytosine basis. We can see

<sup>8</sup>It is important to notice here that the total energy and forces calculated using this configuration cannot be considered accurate.

that the HOMO (A in figure (5.8)) is clearly dominated by the Guanine states ( $\sim 1$  eV below  $E_F$ ). One can notice that the broad occupied molecular orbital (BOMO) identified as (B) in the figure includes some contribution from the backbone and the pentose. Finally the LUMO is mostly dominated by Cytosine and the HOMO-LUMO gap is approximately 2 eV.

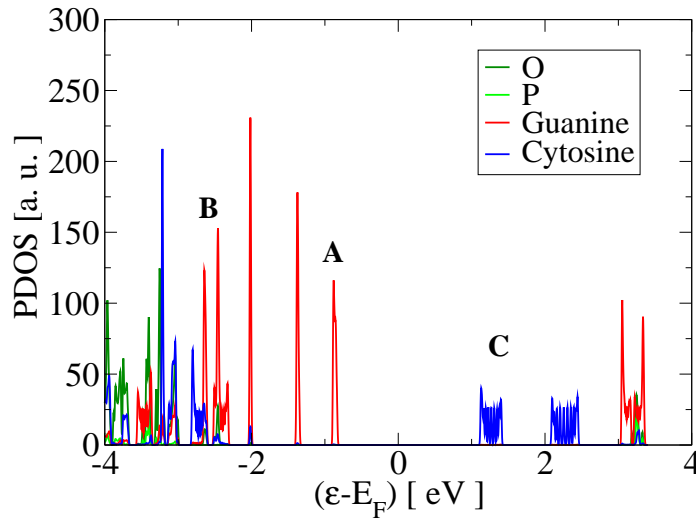


Figure 5.8: Total and partial density of states for infinite double-stranded Poly-(dC)-Poly-(dG) A-DNA. The partial density of states has been projected on either the Guanine or the Cytosine basis. Three states have been indicated: A) the HOMO, B) broad occupied molecular orbital (BOMO), and C) the LUMO.

This can be further corroborated by looking at the charge density projected onto these states. These are plotted in figure (5.9). Notably the delocalised  $\pi$  states over the Guanine are accountable for the HOMO while we see some charge density on the pentose and the phosphate backbone for the BOMO.

These results are similar to those obtained by Taniguchi and Tomoji [247] for infinite DNA double strands.

### 5.2.3 Two-base-pair DNA

We start our transport calculations *per se* by considering the small DNA complex. We performed extensive atomic conjugate gradient relaxations to obtain the optimised structure. In particular we are interested in obtaining the correct position of the sulphur atoms on the gold surface. We found that the distance between the S atoms and the surface is  $2.5 \text{ \AA}$ , similar to those obtained for simpler thiolated

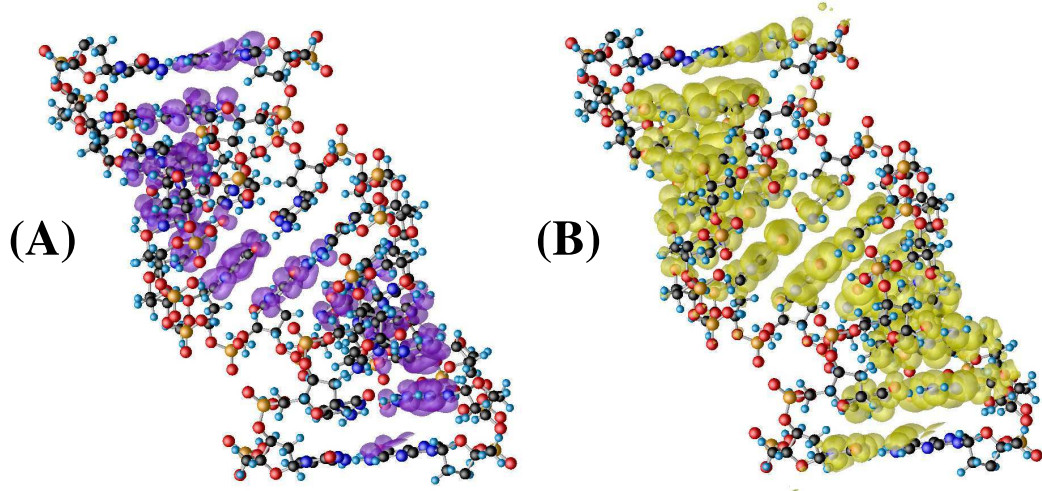


Figure 5.9: Iso-surfaces for local charge density for the (A) HOMO and (B) BOMO as highlighted in figure (5.8). For display purposes we have include one extra base pair totalling 12 base pairs.

compounds [179, 180].<sup>9</sup>

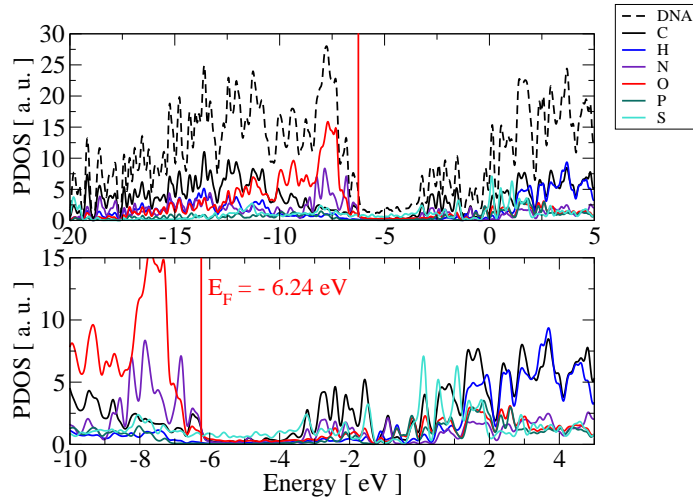


Figure 5.10: (a-b) Projected density of states of a thiolated two-base-pair structure attached to gold electrodes. Top and bottom panels represent the same PDOS with different energy ranges. The vertical red line indicates the position of the Fermi level,  $E_F = -6.24$  eV.

From the projected density of states (Fig. (5.10)) we can clearly see the presence of broad states around the Fermi level. We also note the presence of a broad

<sup>9</sup>For the atomic relaxations we included the  $5d$  and empty  $6p$  orbitals of gold in the valence for all the atoms in the leads.

sulphur state within the molecular gap. By further looking at the charge density projected around  $E_F$  (Fig. (5.11)) we can notice that the charge spreads over the entire molecule. Moreover there is considerable charge around the S end-groups. From this analysis one would expect large conductance, however one cannot say so for sure unless transport calculations are performed.

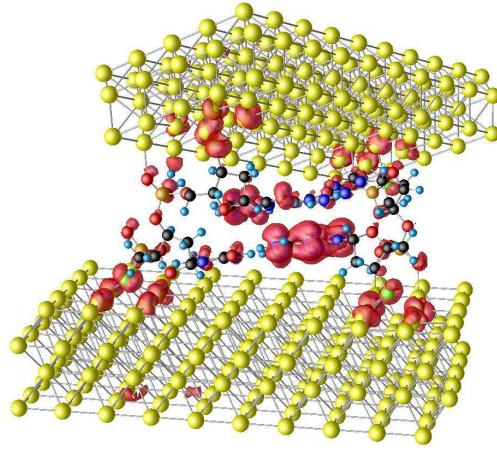


Figure 5.11: Projected charge density around the Fermi level for a two-base-pair DNA molecule attached to gold electrodes. Legend: Au - yellow, C - black, H - light blue, N - blue, O - red, P - orange, S - green.

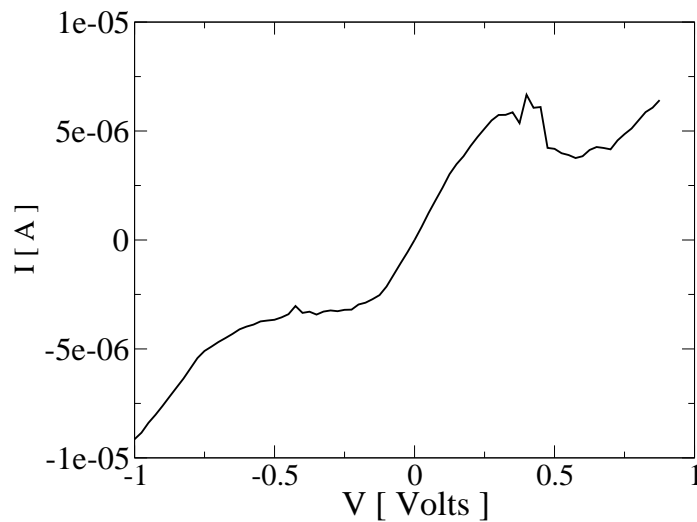


Figure 5.12: Current as a function of bias for a two-base-pair DNA strand. The  $I - V$  is quite asymmetric and the current reaches  $10 \mu\text{A}$  at 1 Volt.

The current as a function of bias for this short DNA strand is shown in figure

(5.12). We can see that the current is close to  $-10 \mu\text{A}$  at  $-1 \text{ V}$  (and  $\sim 7 \mu\text{A}$  at  $1 \text{ V}$ ) and is highly asymmetric. Moreover there is no gap in the  $I - V$ . This behaviour can be understood from inspecting the transmission coefficients as a function of energy for zero bias (Fig. (5.13)). There are two broad resonances close to  $E_F$  and the transmission for these resonances is close to unity. These two resonances can be associated with the pinning of the HOMO to the Fermi level. As we can see from the projected density of states for the entire system, this state is broadened by the interaction with the electrodes. In the presence of an external electric field these resonances will immediately contribute towards the conductance which in turn results in an absence of conduction gaps around zero bias.

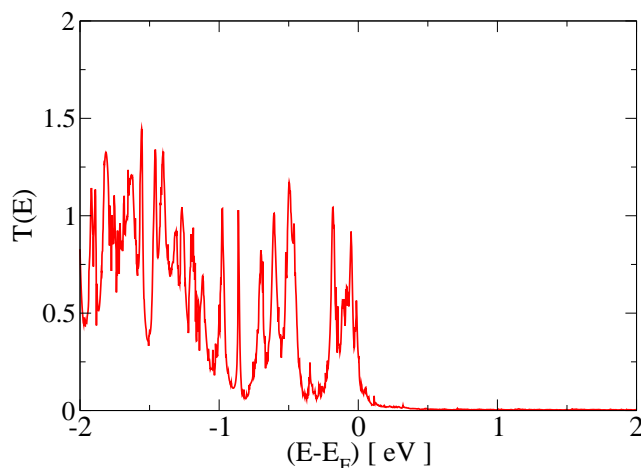


Figure 5.13: Transmission as a function of energy for a two-base-pair attached to gold electrodes.

Since the molecule is so short this behaviour can be associated to direct tunnelling between sulphur surface states. We consider this possibility by performing a calculation where the two-base-pair molecule was entirely removed from the contact region. In order to correctly model the vacuum region where we removed the molecule from we introduced ghost atoms [40].<sup>10</sup> The results for the transmission coefficients at zero bias are shown in figure (5.14). From the figure we can note the presence of a peak slightly below the Fermi level associated to a gold-sulphur surface state. Hence we can conclude that the transport is mainly through sulphur and the molecule merely acts as a medium that effectively lowers the dielectric constant of

<sup>10</sup>The charge density in the vacuum region is usually poorly described by localised-basis-set approaches to DFT because these are usually atom centred. By introducing ghost atoms we include in the calculation extra basis functions in the vacuum region. These extra empty states have the same symmetry of the LCAO's used for the real atoms without including the pseudopotential.



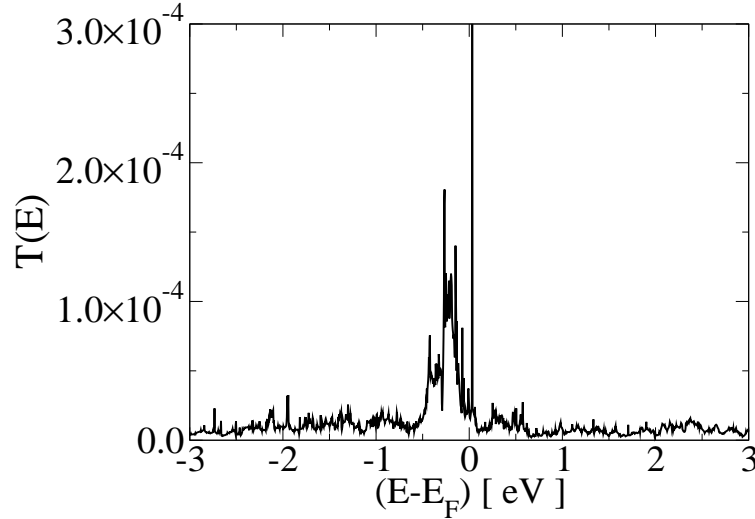


Figure 5.14: Energy dependent transmission coefficients between two [001] gold surfaces with sulphur atoms attached to the hollow sites. The DNA molecule has been removed but we have introduced ghost atoms to model the vacuum region.

the region between the two surfaces.

#### 5.2.4 Transport through A-DNA molecules

For the longer A-Poly(dG)-Poly(dC) DNA molecule attached to gold, the fully relaxed atomic arrangement of the isolated molecule was considered. Those positions were kept fixed while S atoms were attached to the 5' and 3' sites at both ends of the molecule. This arrangement was then allowed to relax in a super cell with no boundary conditions. Subsequently the sulphur end-groups were attached to the hollow site of the [001] Au surface using the sulphur/surface distance obtained in the previous calculations of section (5.2.3).

The projected density of states of the eleven-base-pair A-DNA molecule is shown in figure (5.15). The picture shows features reminiscent of the isolated molecule. Most notably signatures of the HOMO, the LUMO and the gap remain largely unaffected after attachment to the electrodes. While we saw a broad sulphur state across the entire gap in section (5.2.3), here region identified as the HOMO-LUMO gap of the isolated molecule (  $[-5.14, -2.8]$  eV ) is practically devoid of states.

As it was the case with the two-base pair molecule the Fermi level is pinned to the HOMO of the isolated molecule. However, we can clearly see that that state is now much sharper. In other words, not as strongly coupled. The PDOS starts to broaden  $\sim 1.5$  Volts below the Fermi level where oxygen states become important.



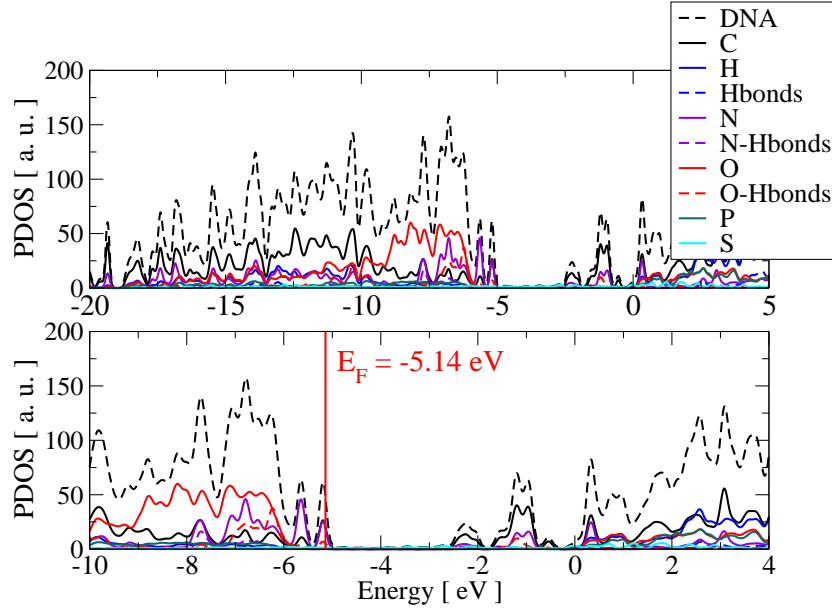


Figure 5.15: Projected density of states of a thiolated A-DNA structure attached to gold electrodes. Top and bottom panels correspond to the same system with different energy range.

By projecting the charge density around the Fermi level we can clearly see that most of the contribution to this energy region comes from the HOMO of the isolated molecule with some effect from the anchoring sulphur atoms.

The total transmission coefficients show some interesting behaviour. While the PDOS shows that the Fermi level is pinned to the HOMO we find very little conductance around  $E_F$ .

The HOMO is almost completely decoupled. In other words, although the HOMO is mostly due to the Guanine  $\pi$  states, the coupling between planes is close to zero as suggested by [238]. We can see that the transmission starts to be significant around 1.5 eV below the Fermi level. In the Landauer-Büttiker approach this would mean that an external applied bias of approximately 3 Volts would lead to coherent band conduction.

Hence, while calculations for the isolated molecule give some indication of the transport properties of these systems, only fully *ab initio* transport calculations where the effects of the electrodes are taken into consideration can elucidate the full quantum mechanical transport properties of these macromolecules.

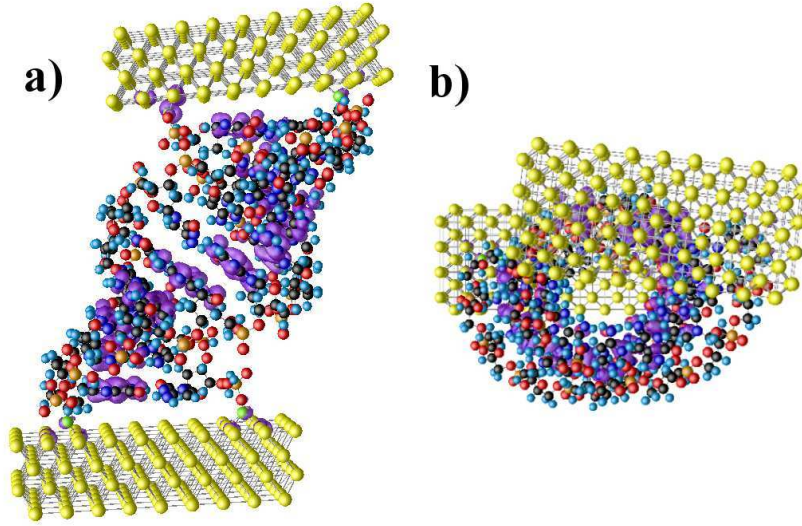


Figure 5.16: Iso-surface plot of the local density around the Fermi level. a) Side view and b) top view. The charge around the Fermi level is concentrated in the Guanine basis. Legend: Au - yellow, H - light blue, C - black, N - blue, O - red, P - orange, S - green.

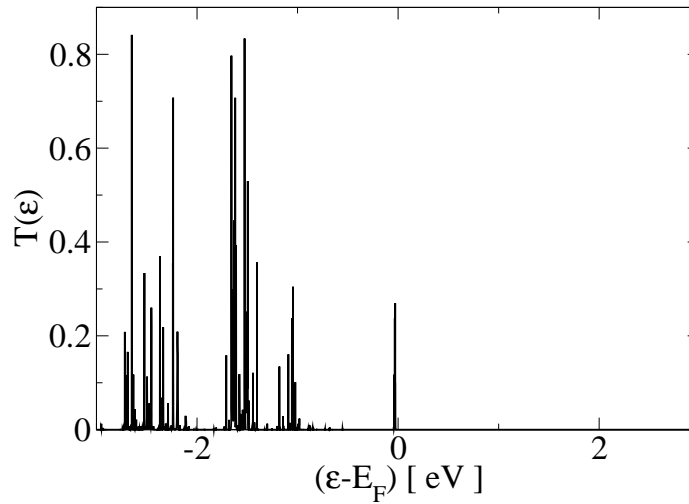


Figure 5.17: Transmission as a function of energy for a 11-base pair DNA strand attached to gold electrodes.

### 5.3 Conclusions

As we have seen, for both the short and long DNA molecules, the Fermi level is pinned to the HOMO as soon as we attach the electrodes. However, while in the short DNA the HOMO is broadened by coupling to the electrodes, the largely Guanine-

dominated HOMO level in the long DNA molecule is very localised. In that case, the HOMO is represented by a series of uncoupled states sitting in each of the Guanine bases.

Previous calculations [248] have shown that this effect would be present due to symmetry in A-DNA corroborating our results.

The broadened states in the short DNA molecule leads to high conductance even at zero bias, so once the bias is increased we see a large current response. On the other hand, the transmission coefficients of the long DNA show a clear gap up to 1.5 eV around the Fermi level. The gap leads to a flat  $I - V$  characteristics up to 3 Volts. After that we clearly see conductance. This result is in agreement with a band transport mechanism through a wide band-gap semiconductor.

This result is completely consistent with experimental results in dry short DNA double strands performed by Cohen *et. al.*. We can clearly see that the states responsible are not the HOMO neither they correspond to the LUMO. The broader states responsible for the conductance lie below the HOMO in the so called BOMO state. This is related to the backbone instead of the basis. This leads us to believe that the transport properties of DNA are largely independent of our basis choice. In that case, it is also very robust with respect to localisation effects.

